

# Mechanical Implementation of Postural Synergies of an Underactuated Prosthetic Hand

Kai Xu<sup>1</sup>, Yuheng Du<sup>1</sup>, Huan Liu<sup>1</sup>, Xinjun Sheng<sup>2</sup>, and Xiangyang Zhu<sup>2</sup>

<sup>1</sup> RII Lab (Lab of Robotics Innovation and Intervention), UM-SJTU Joint Institute,

<sup>2</sup> Robotics Institute, School of Mechanical Engineering

Shanghai Jiao Tong University,

Shanghai, 200240, China

{k.xu, dyh, h.liu, xjsheng, mexyzhu}@sjtu.edu.cn

**Abstract.** Recent advances in neurology showed that human controls dozens of muscles for hand motions in a coordinated manner. Such coordination is referred as to a postural synergy and synergies could be combined to form various hand poses. Implementing the synergies digitally in the controller, 6 to 12 motors of a robotic prosthetic hand can be controlled by a few synergy inputs from an amputee's bio-signal interfaces. This paper proposes to implement the synergies via a mechanical transmission unit so that two rotation inputs can be scaled, combined and mapped to 13 rotary outputs to enable not only grasping but also manipulation of a prosthetic hand. Synthesis of the postural synergies and design of the prosthetic hand are briefly reviewed, whereas the transmission design is elaborated as the implementation of the postural synergies. Tests were performed to quantify how well the synergies could be reproduced via the transmission. Experiments that follows are expected to demonstrate the effectiveness of constructing a low cost yet versatile prosthetic hand by mechanically implementing the postural synergies.

**Keywords:** Prosthetic hand, postural synergies, underactuated mechanisms, planetary gears.

## 1 Introduction

It is a challenging task to construct an anthropomorphic prosthetic hand that can reproduce the delicate motions of the biological original. In order to achieve this goal, the prosthetic hand shall be versatile enough for various daily tasks and controllable through a bio-signal interface, such as EMG (electro-myography) or EEG (electro-encephalography). However limited bandwidth of these interfaces used to prevent fully actuated robotic hands from being applied as prostheses if each DoF (Degree of Freedom) requires individual control, even though many designs were absolutely the state-of-the-art (e.g. the ones in [1-4]).

Recent advances in neurology suggested a possible way of achieving dexterous control of a prosthetic hand via limited inputs. It was showed that CNS (Central Nervous System) controls dozens of muscles for hand poses in a coordinated manner.

Such coordination is referred as to a postural synergy, which corresponds to flexion and/or extension actuation statuses of the involved muscles. CNS combines postural synergies, adjusting each synergy's coefficient (weight), to realize various hand motions. Combination of two primary postural synergies accounts for about 84% of the variance of dozens of different grasping postures [5]. What's more, CNS switches between different sets of postural synergies for distinct grasping and manipulations tasks [6].

These findings have led to the application of a robotic hand with many actuators as prosthesis. Two channels of the bio signals as synergy inputs would act as coefficients while combining two postural synergies. Several existing designs have practiced this idea, such as the DLR II Hand with two synergies [7], the SAH hand with three synergies [8], the UB hand with two synergies [9], and the ACT hand which uses two and three postural synergies to control 24 actuators to perform writing and piano playing [10, 11]. The aforementioned designs are certainly functional but the cost of such a prosthetic hand could also be quite high (multiple sets of miniature servomotors with amplifiers, feedback sensors and controllers). If postural synergies could be mechanically implemented, such a prosthetic hand could potentially be more affordable with a low cost.

Mechanical implementation of postural synergies was attempted by Brown and Asada using differential pulleys [12]. Various postures of the hand were formed. However, grasping performance and effectiveness of the mechanically implemented postural synergies were not studied. This paper proposes a different approach to realize the mechanical implementation of the postural synergies using planetary gears. Positive results of this paper could prove the effectiveness of implementing postural synergies mechanically.

Synthesis of the postural synergies are briefly summarized in Section 2, which was detailed in [13]. Mechanism designs of the prosthetic hands and the transmission as a mechanical implementation of the posture synergies are elaborated in Section 3. Tests and experiments are presented in Section 4 with conclusions and future work followed in Section 5.

## 2 Postural Synergy Synthesis

Unlike referring to the discrete grasp taxonomy as in [14-16], using the postural synergies introduced a new way to reproduce various hand grasping motions. As shown in a milestone work by Ciocarlie and Allen [17], poses of several different hands were optimized to achieve various grasping tasks. Since two synergy inputs can be optimized for the grasping of distinct objects, they could also be used to perform manipulation of the same object (manipulating one object is essentially a smooth transition between consecutive grasping patterns of the same object). It's possible to upgrade the motion capability of a prosthetic hand from grasping to manipulation using the concept of the postural synergies.

The postural synergies are usually extracted as the first two principal components from a series recorded hand poses. If the synergies are implemented digitally, the controller would map the two synergy inputs  $q_1$  and  $q_2$  to the actuator outputs  $\mathbf{p}$

as shown in Eq. (1), where  $\mathbf{u}_1$  and  $\mathbf{u}_2$  are the postural synergies, and  $\bar{\mathbf{p}}$  is an average output. If the prosthetic hand has  $n$  actuators,  $\mathbf{p}$ ,  $\mathbf{u}_1$ ,  $\mathbf{u}_2$  and  $\bar{\mathbf{p}}$  are all  $n \times 1$  vectors.

$$\mathbf{p} = \bar{\mathbf{p}} + q_1 \mathbf{u}_1 + q_2 \mathbf{u}_2 \quad (1)$$

While performing grasping tasks as in [7-9, 17], the synergy inputs were optimized to properly form poses of the hand. As a matter of fact, these adjustments essentially compensated for the discrepancy between the original postural synergies and their implementations. While planning a manipulation task for a prosthetic hand, the synergy inputs will be mainly used to transform the hand from one pose to another in a continuous manner, limiting their roles in compensating the implemented postural synergies. Hence, the synergy discrepancy should be minimized to satisfactorily reproduce the specific sequenced motions via only two synergy inputs.

In order to minimize the synergy discrepancy, this paper introduces a novel technique of synthesizing the postural synergies by constructing a dummy hand. Instead of inviting 5 to 10 human subjects, asking them to manipulate one or more objects, recording and analyzing the human hand motions using sophisticated systems such as CyberGlove™ or the Vicon™ cameras, this dummy hand was constructed and manually posed for manipulation tasks with each pose measured. Constructing a dummy hand and measuring its poses could produce direct results for the synergy synthesis in a very cost-efficient way. More importantly it avoided unnecessary errors while designing prosthetic mechanisms with lower kinematic pairs (e.g. revolute joints) based on measurements of human hands whose joints are essentially higher kinematic pairs (e.g. the carpometacarpal joint, the metacarpophalangeal joints).

The dummy hand was constructed as in Fig. 1-(a). All the joints were passive with enough friction against external disturbance (e.g. gravity). The arrangement of its revolute joints provided motion capabilities similar to a human hand. The joints are named as follows. Letters *T*, *M*, *R*, *L* and *I* before the underscore indicate the joints for the thumb, the middle finger, the ring finger and the little finger respectively. Abbreviations of *rot*, *mcp*, *ip*, *abd*, *pip* and *dip* after the underscore indicate the rotation joint, the metacarpophalangeal joint, the interphalangeal joint, the abduction joint, the proximal and the distal interphalangeal joint respectively.

The specific motion paradigm is the manipulation of two rehabilitation training balls on the palm in a cyclic way, as shown in Fig. 1. This exercise helps the seniors or mild-stroke patients to maintain or recover their hand motor function. Although this paradigm might not seem practically meaningful to amputees, the motivation is to demonstrate the effectiveness of this presented synergy synthesis.

In each pose, joint angles were measured using an optical tracker (MicronTracker SX60 from Claron Technology Inc) as shown in Fig. 1-(b). The two intersecting surfaces of the two adjacent phalanxes were first characterized by obtaining coordinates of three points on the surfaces. The joint angle was then obtained from the dot product of the two surface normals. Six key poses as in Fig. 1-(c) to Fig. 1-(h) are identified and recorded. With detailed processes and numerical values available in [13], results of the postural synergies are briefly summarized.

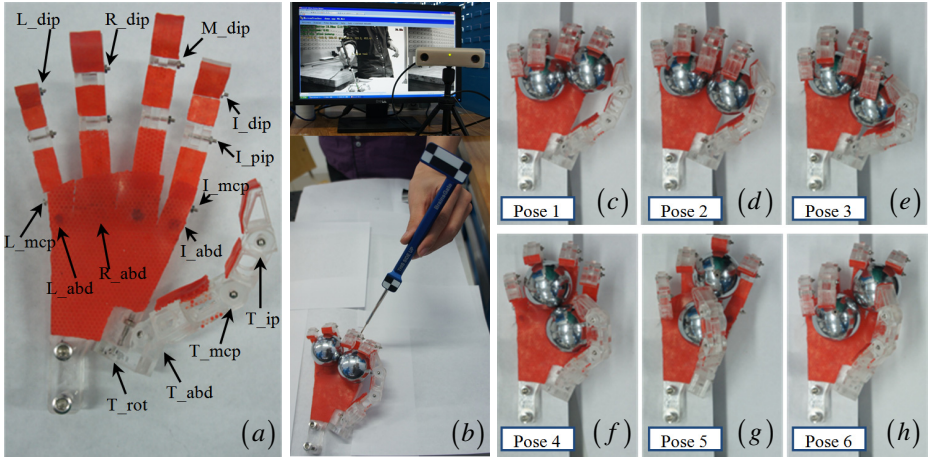


**Fig. 1.** The dummy and its poses: (a) construction, (b) measurement process of the joint angles using an optical tracker, (c) to (h) six key poses for manipulating two training balls

Each pose in Fig. 1-(c)~(h) corresponds to a pose vector  $\mathbf{p}_i \in \mathfrak{R}_{19 \times 1}$ ,  $i = 1, 2, \dots, 6$ . Since motions of the four distal interphalangeal joints (I\_dip, M\_dip, R\_dip and L\_dip) were coupled to the motions of the four proximal interphalangeal joints (I\_pip, M\_pip, R\_pip and L\_pip), dimension of the pose vector can be reduced,  $\mathbf{p}_i \in \mathfrak{R}_{15 \times 1}$ .

Six poses in Fig. 1-(c)~(h) can be put side to side to form a pose matrix  $\mathbf{P}$ . Singular value decomposition of the pose matrix  $\mathbf{P}$  is as in Eq. (2).

$$\begin{aligned}
 \mathbf{P}_{15 \times 6} &= [\mathbf{p}_1 \quad \mathbf{p}_2 \quad \dots \quad \mathbf{p}_6] = \bar{\mathbf{P}} + \mathbf{U}_{15 \times 15} \boldsymbol{\Sigma}_{15 \times 6} \mathbf{V}_{6 \times 6}^T \\
 &= \bar{\mathbf{P}} + [\mathbf{u}_1 \quad \mathbf{u}_2 \quad \dots \quad \mathbf{u}_{15}] \cdot \begin{bmatrix} \text{diag}(\delta_1, \delta_2, \dots, \delta_6) \\ \mathbf{0}_{9 \times 6} \end{bmatrix} \begin{bmatrix} \mathbf{v}_1^T \\ \mathbf{v}_2^T \\ \vdots \\ \mathbf{v}_6^T \end{bmatrix}. \tag{2}
 \end{aligned}$$

Where  $\bar{\mathbf{P}} = [\bar{\mathbf{p}} \quad \bar{\mathbf{p}} \quad \bar{\mathbf{p}} \quad \bar{\mathbf{p}} \quad \bar{\mathbf{p}} \quad \bar{\mathbf{p}}]$  is the average pose and  $\bar{\mathbf{p}} = \frac{1}{6} \sum_{i=1}^6 \mathbf{p}_i$ .

By neglecting the singular values  $\delta_i$  ( $i = 3, 4, 5, 6$ ), hand poses (the pose matrix  $\tilde{\mathbf{P}}$  and the individual pose vector  $\tilde{\mathbf{p}}_i$ ) can be reproduced as in Eq. (3) and Eq. (4). Vectors  $\mathbf{u}_1$  and  $\mathbf{u}_2$  are referred to as the postural synergies. With  $q_{1i}$  and  $q_{2i}$  as synergy inputs, various hand poses could be approximated. The average pose vector

$\bar{\mathbf{p}}$ , the postural synergies  $\mathbf{u}_1$  and  $\mathbf{u}_2$ , and inputs  $q_{ki}$  ( $k=1,2$  and  $i=1,2,\dots,6$ ) are summarized in Table 1.

$$\tilde{\mathbf{P}} = \bar{\mathbf{P}} + [\mathbf{u}_1 \quad \mathbf{u}_2] \begin{bmatrix} \delta_1 \mathbf{v}_1^T \\ \delta_2 \mathbf{v}_2^T \end{bmatrix} = \bar{\mathbf{P}} + [\mathbf{u}_1 \quad \mathbf{u}_2] \begin{bmatrix} q_{11} & q_{12} & \cdots & q_{16} \\ q_{21} & q_{22} & \cdots & q_{26} \end{bmatrix}. \quad (3)$$

$$\tilde{\mathbf{p}}_i = \bar{\mathbf{p}} + q_{1i}\mathbf{u}_1 + q_{2i}\mathbf{u}_2, \quad i = 1, 2, \dots, 6. \quad (4)$$

**Table 1.** The average pose, the postural synergies and the synergy inputs

Joints	Average pose (°)	Postural synergies		Synergy inputs (°)
		$\mathbf{u}_1$	$\mathbf{u}_2$	
T_rot	59.7	-0.49	0.24	$q_{11} = 36.2^\circ$
T_mcp	38.7	-0.16	-0.21	$q_{21} = 21.0^\circ$
T_ip	44.0	-0.15	-0.23	$q_{12} = 28.1^\circ$
T_abd	43.0	-0.2	-0.17	$q_{22} = -1.1^\circ$
L_mcp	44.8	0.34	-0.66	$q_{13} = 37.6^\circ$
M_mcp	28.2	0.56	0.12	$q_{23} = -31.5^\circ$
R_mcp	35.8	0.44	0.5	$q_{14} = -38.5^\circ$
L_mcp	58.3	0.15	-0.25	$q_{24} = -25.1^\circ$
L_pip	54.8	0.01	0.06	$q_{15} = -52.4^\circ$
M_pip	72.0	-0.01	-0.11	$q_{25} = 2.6^\circ$
R_pip	72.5	-0.02	0.08	$q_{16} = -11.0^\circ$
L_pip	70	-0.13	0.14	$q_{26} = 34.1^\circ$
I_abd	8.7	0.03	0.08	
R_abd	9.7	-0.05	-0.02	
L_abd	15.5	-0.02	0.07	

### 3 Design Descriptions of the Prosthetic Hand

#### 3.1 Design Overview

This paper proposes to implement postural synergies mechanically. According to Eq. (4), a pair of synergy control inputs  $q_{1i}$  and  $q_{2i}$  shall be combined and scaled, then mapped to the outputs through a transmission to drive the prosthetic hand from its average pose  $\bar{\mathbf{p}}$ . This transmission is referred as to the mechanical implementation of the postural synergies.

This mechanical implementation of synergies could be installed in forearm since it is unlikely such a complicated transmission could be fully embedded in palm. All the outputs from the transmission will be connected to the prosthetic hand to drive the finger joints using flexible shafts, as shown in Fig. 2. Decisions on i) how to realize the mechanical implementation of synergies, ii) how to actuate finger joints, and iii) how to connect the transmission outputs to the finger joint axes, should be made consistently and compatibly.

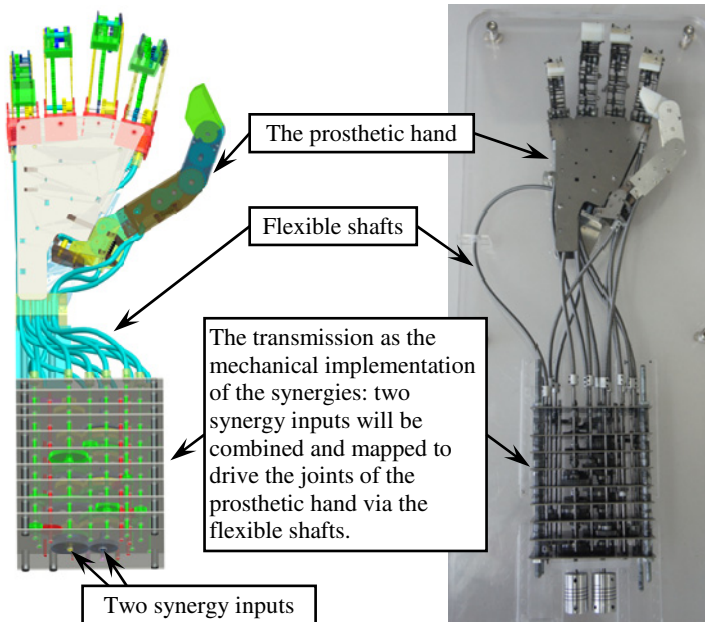


**Fig. 2.** Design overview of the prosthetic hand and the mechanical synergy implementation

Since inputs  $q_{1i}$  and  $q_{2i}$  ( $i = 1, 2, \dots, 6$ ) shall be combined and scaled, there are only a few options to realize this function mechanically. Possible options include designing a differential hydraulic system, using differential pulleys (as in [12]), using planetary gears, etc. This paper chose to use planetary gears because this option might provide better accuracy than that of using differential pulleys and might be easier to fabricate than that of designing a differential hydraulic system. Then the synergy outputs will be rotations (instead of being translations as in the other two options). The most direct way to connect these synergy outputs to the finger joint axes is to use flexible shafts. What's more, rotations of these flexible shafts would not be affected by a future presence of possible wrist motions. Using worm gears and gears, rotations of these flexible shafts will drive all the finger joints.

Section 3.2 summarizes the transmission and actuation designs of the prosthetic hand which were detailed in [13], whereas Section 3.3 elaborates the design of the

mechanical implementation of synergies. The prosthetic hand and the mechanical synergy implementation were then fabricated, assembled and connected. Two actuators are expected to drive all the joints of the prosthetic hand to realize the desired motion sequence.

### 3.2 Design of the Prosthetic Hand

As shown in Fig. 3, several flexible shafts were connected to the worms to the drive worm gears. Then the worm gears were attached to a train of spur gears to actuate the hand joints. The train of spur gears was used to allow proper positioning of the worms and worm gears so that they could be fully housed inside the thumb. All the worm gears used had a gear ratio of 20:1.

As shown in Fig. 3-(a), a dual arrangement of worm gears introduced coupling between the  $T_{mcp}$  and the  $T_{ip}$  joints. Once the worm gear for the  $T_{mcp}$  joint was actuated, in order to keep the thumb distal phalanx stationary with respect to the thumb proximal phalanx, the worm gear for the  $T_{ip}$  joint should be actuated accordingly. This coupling should be accommodated while designing the transmission.

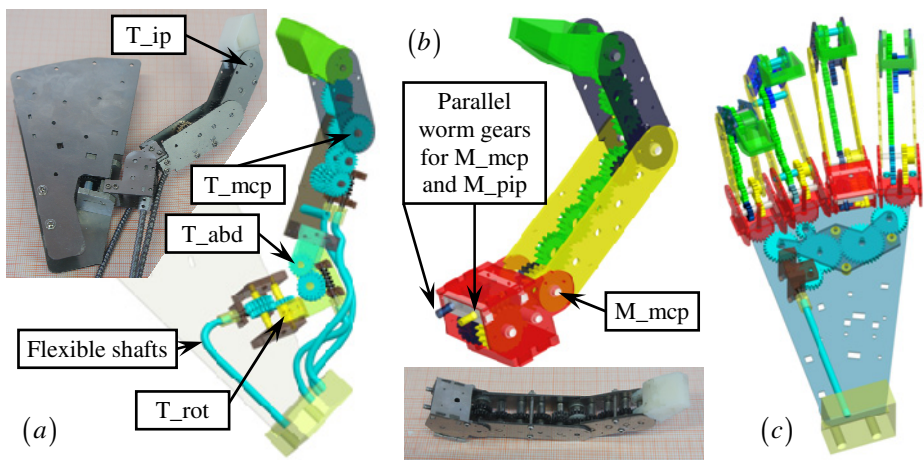


**Fig. 3.** Design of the prosthetic hand: (a) structure of the thumb, (b) structure of the middle finger, and (c) the structure for the abduction of the fingers

Similar to the actuation of the thumb joints, flexible shafts were connected to the worms and the spur gears to drive the metacarpophalangeal and interphalangeal joints. Since actuation of the index, the middle, the ring and the little fingers are essentially similar, Fig. 3-(b) only shows the structure of the middle finger. Coupling between the distal interphalangeal joint and the proximal interphalangeal joint was realized using trains of spur gears inside the fingers. Axes of these gears were offset to accommodate their specific pitch radiuses.

According to Eq. (4) and Table 1, abduction motions of the index, the ring and the little fingers were also subjected to inputs  $q_{1i}$  and  $q_{2i}$ . However, their synergies values (abd rows for  $\mathbf{u}_i$ ) are substantially smaller than those of other joints. In order to reduce the complicity of the transmission, abduction motions of the three fingers were made coupled. Gear profiles were fabricated on components of the finger subassemblies so that one set of worm & worm gear will drive abduction motions of the index, the ring and the little fingers through a train of spur gears.

### 3.3 Implementation of the Postural Synergies via a Mechanical Transmission

This paper proposes to implement the postural synergies mechanically. In other words, two synergy inputs will be scaled, combined and mapped to the synergy outputs through a mechanical transmission unit. Due to the coupling between the four distal interphalangeal joints and the respective proximal interphalangeal joints, 19 joints of the prosthetic hand originally required 15 synergy outputs from the transmission. The abduction motions of the index, the ring and the little fingers were made coupled and hence these three joints only required one synergy output. In total, 13 synergy outputs would be needed to drive the prosthetic hand. All the synergy outputs will be connected to the corresponding worms using flexible shafts.

A schematic of the planetary-gear-based transmission for the implementation of the postural synergies is shown in Fig. 4. Two inputs  $q_1$  and  $q_2$  were shared by multiple sets of planetary gears.  $q_2$  was connected to all the sun gears, while  $q_1$  was connected to all the ring gears (annuluses). Idlers were added to make up for the distance between the two input axes. Rotations of the planet carriers were used as outputs which were connected to joint worms through the flexible shafts.

An overall transmission can be derived as in Eq. (5), where  $q_o$  is a synergy output,  $z_i$  and  $z_{ki}$  are the numbers of the indicated gear teeth. The gear teeth can be adjusted so that Eq. (5) is consistent with the numerical values from Table 1.

$$q_o = -\frac{z_5 z_3}{z_6 z_4} \frac{z_1 (z_{k1} + 2z_{k2}) q_1 + z_{k2} q_2}{2(z_{k1} + z_{k2})} . \quad (5)$$

## 4 Preliminary Experiments and Tests

All the components of the prosthetic hand were fabricated and assembled. Four rotations are needed for the T\_rot, the T\_abd, the T\_mcp and the T\_ip joints of the thumb. Two rotations are needed for the metacarpophalangeal joint and the proximal interphalangeal joint of the four fingers (their distal interphalangeal joints are actuated by the proximal interphalangeal joints though couple gear trains). One more rotation

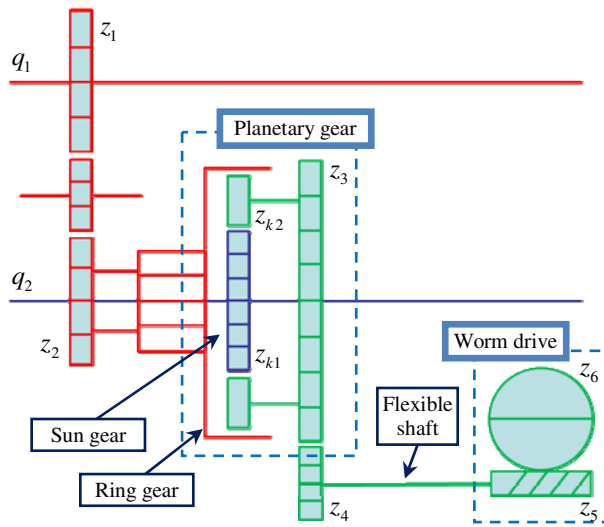


**Fig. 4.** A schematic of the transmission as a mechanical synergy implementation

is needed for the abductions of the fingers. In total, 13 rotational outputs are needed from the transmission to drive the 19 joints in the prosthetic hand (abduction of the middle finger is fixed).

**4.1 Motion Capabilities of the Hand**

The prosthetic hand was manually posed by rotating its flexible shafts, to verify motion ranges of the joints as in Fig. 5. It can be seen that the prosthetic hand can be successfully posed for the six key postures which are needed for manipulating the two rehabilitation training balls.

The experiments performed here only tried to show motion ranges of the prosthetic hand design to qualitatively verify its capability for this intended task. Since the manual actuation of the flexible shafts doesn't correspond to the coupled outputs from the transmission, these poses are naturally different from the ones shown in Fig. 1.

**4.2 Transmission Error Quantification**

The transmission as the mechanical implementation of the postural synergies was designed, fabricated and assembled as a set of planetary gears, as shown in Fig. 6.

Two Maxon DC servomotors were controlled by a Matlab xPC Target to drive the two synergy inputs. Motion control cards included the D/A card PCL-727 from the AdvanTech Inc and the counter card CNT32-8M from the Contec Inc. The synergy outputs were examined one by one using an encoder. Readings from the encoder for one synergy output was plotted with respect to the two synergy inputs, as in Fig. 7.

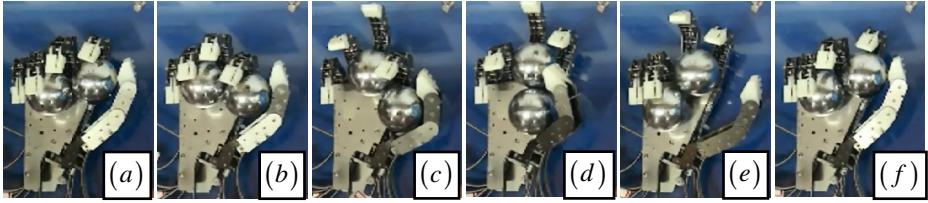


**Fig. 5.** The assembled prosthetic hand was manually posed by rotating the flexible shafts to qualitatively verify its motion capability for the intended task of manipulating two training balls

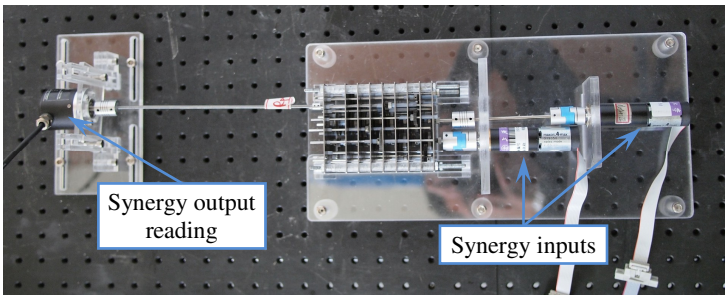


**Fig. 6.** An experimental setup for quantifying transmission errors of the planetary gears

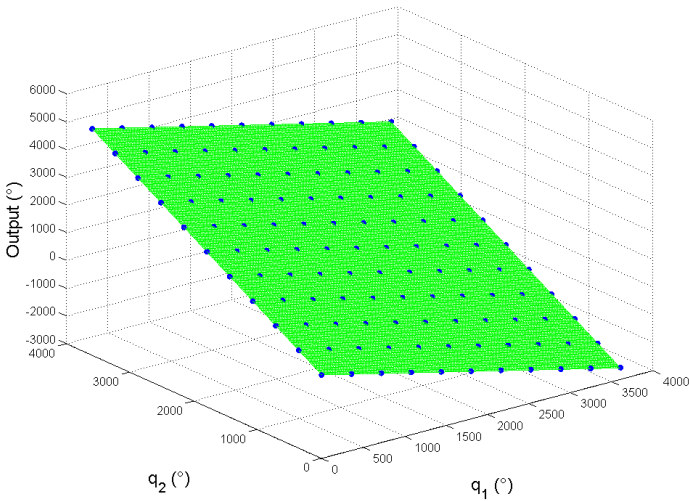


**Fig. 7.** The synergy output with respect to the two synergy inputs

According to the Eq. (4), a synergy output can be visualized as a plane while plotted with respect to the two synergy inputs, which could be seen in Fig. 7. The blue dots represent the measured rotary outputs. The distances between the dots and the plane are transmission errors. According to the experiments, all the errors have been kept under 0.25%. These errors come from the backlash of the gear system.

## 5 Conclusions and Future Work

This paper presents the latest results of a prosthetic hand project regarding the mechanical implementation of the postural synergies, summarizing the structural design and the postural synergy synthesis from previously published results. This project attempts to upgrade motion capability of a prosthetic hand from object grasping to more delicate motions (such as manipulation of objects) using the concept of the postural synergies. A specific manipulation paradigm is the manipulation of two rehabilitation training balls in a cyclic manner using two synergy inputs.

The postural synergies synthesized from several key poses of a dummy hand were implemented mechanically via a transmission unit. The transmission unit combines, scales and maps two synergy inputs to 13 synergy outputs and the outputs are routed to the prosthetic hand via flexible shafts to drive the prosthetic hand. The transmission unit was tested through a series of experiments and the transmission errors were quantified.

Future work includes several aspects. The first aspect is to further improve the kinematic performance of the prosthetic hand. Currently the hand joints have quite some backlash which should be eliminated by preloading the joints using a spring. Secondly inter-pose planning of the synergy inputs will be investigated, trying to realize the proposed manipulation task in a continuous manner. Thirdly, motion capabilities of additional grasping and manipulating tasks will be explored using the same transmission and the prosthetic hand.

**Acknowledgments.** This work was supported by the Chinese National Program on Key Basic Research Projects (the 973 Program) #2011CB013300.

## References

1. Bicchi, A.: Hands for Dexterous Manipulation and Robust Grasping: a Difficult Road toward Simplicity. *IEEE Transactions on Robotics and Automation* 16(6), 652–662 (2000)
2. Gazeau, J.P., Zeghloul, S., Arsicault, M., Lallemand, J.P.: The LMS Hand: Force and Position Controls in the Aim of the Fine Manipulation of Objects. In: *IEEE International Conference on Robotics and Automation (ICRA)*, Seoul, Korea (2001)
3. Liu, H., Meusel, P., Seitz, N., Willberg, B., Hirzinger, G., Jin, M.H., Liu, Y.W., Wei, R., Xie, Z.W.: The Modular Multisensory DLR-HIT-Hand. *Mechanism and Machine Theory* 42(5), 612–625 (2007)
4. Grebenstein, M., Chalon, M., Friedl, W., Haddadin, S., Wimböck, T., Hirzinger, G., Siegart, R.: The Hand of the DLR Hand Arm System: Designed for Interaction. *International Journal of Robotics Research* 31(13), 1531–1555 (2012)

5. Santello, M., Flanders, M., Soechting, J.F.: Postural Hand Synergies for Tool Use. *The Journal of Neuroscience* 18(23), 10105–10115 (1998)
6. Weiss, E.J., Flanders, M.: Muscular and Postural Synergies of the Human Hand. *Journal of Neurophysiology* 92(1), 523–535 (2004)
7. Wimböck, T., Jahn, B., Hirzinger, G.: Synergy Level Impedance Control for Multifingered Hands. In: *IEEE/RSJ International Conference on Intelligent Robots and Systems (IROS)*, San Francisco, CA, USA, pp. 973–979 (2011)
8. Rosell, J., Suárez, R., Rosales, C., Pérez, A.: Autonomous Motion Planning of a Hand-Arm Robotic System Based on Captured Human-like Hand Postures. *Autonomous Robots* 31(1), 87–102 (2011)
9. Ficuciello, F., Palli, G., Melchiorri, C., Siciliano, B.: Experimental evaluation of Postural Synergies during Reach to Grasp with the UB Hand IV. In: *IEEE/RSJ International Conference on Intelligent Robots and Systems (IROS)*, San Francisco, CA, USA, pp. 1775–1780 (2011)
10. Rombokas, E., Malhotra, M., Matsuoka, Y.: Task-specific Demonstration and Practiced Synergies for Writing with the ACT Hand. In: *IEEE International Conference on Robotics and Automation (ICRA)*, Shanghai, China, pp. 5363–5368 (2011)
11. Zhang, A., Malhotra, M., Matsuoka, Y.: Musical Piano Performance by the ACT Hand. In: *IEEE International Conference on Robotics and Automation (ICRA)*, Shanghai, China, pp. 3536–3541 (2011)
12. Brown, C.Y., Asada, H.H.: Inter-Finger Coordination and Postural Synergies in Robot Hands via Mechanical Implementation of Principal Components Analysis. In: *IEEE/RSJ International Conference on Intelligent Robots and Systems (IROS)*, San Diego, CA, USA, pp. 2877–2882 (2007)
13. Xu, K., Zhao, J., Du, Y., Zhu, X.: Design and Postural Synergy Synthesis of a Prosthetic Hand for a Manipulation Task. In: *IEEE/ASME International Conference on Advanced Intelligent Mechatronics (AIM)*, Wollongong, Australia (2013)
14. Cutkosky, M.R.: On Grasp Choice, Grasp Models, and the Design of Hands for Manufacturing Tasks. *IEEE Transactions on Robotics and Automation* 5(3), 269–279 (1989)
15. Feix, T., Pawlik, R., Schmiedmayer, H.-B., Romero, J., Kragić, D.: A Comprehensive Grasp Taxonomy. In: *Robotics, Science and Systems Conference (RSS)*, Seattle, Washington, USA (2009)
16. Zheng, J.Z., De La Rosa, S., Dollar, A.M.: An Investigation of Grasp Type and Frequency in Daily Household and Machine Shop Tasks. In: *IEEE International Conference on Robotics and Automation (ICRA)*, Shanghai, China, pp. 4169–4175 (2011)
17. Ciocarlie, M.T., Allen, P.K.: Hand Posture Subspaces for Dexterous Robotic Grasping. *The International Journal of Robotics Research* 28(7), 851–867 (2009)